

Formation Mechanism of Iodinated Aromatic Disinfection Byproducts: Acid Catalysis with H_2OI^+

Yanpeng Gao,^{||} Junlang Qiu,^{||} Yuemeng Ji, Nicholas J. P. Wawryk, Taicheng An,* and Xing-Fang Li*



Cite This: *Environ. Sci. Technol.* 2022, 56, 1791–1800



Read Online

ACCESS |



Metrics & More



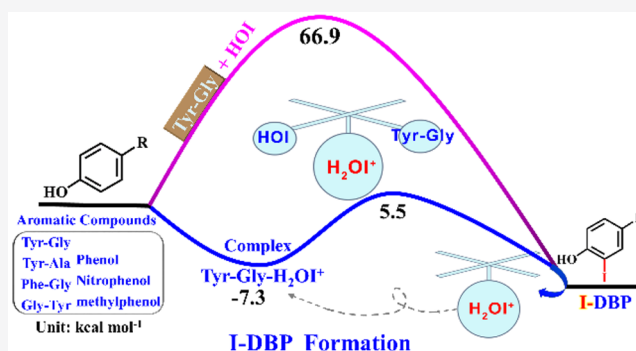
Article Recommendations



Supporting Information

ABSTRACT: Iodinated aromatic disinfection byproducts (I-DBPs) are a group of nonregulated but highly toxic DBPs. The formation of I-DBPs is attributed mainly to HOI because it is the most abundant reactive iodine species in chloraminated water. In this study, we used computational modeling of thermodynamics to examine the mechanism of iodination of aromatic contaminants, e.g., dipeptides and phenols. Computational prediction of the energy barriers of the formation of iodinated tyrosylglycine (I-Tyr-Gly) ($66.9 \text{ kcal mol}^{-1}$) and hydroxylated Tyr-Gly (OH-Tyr-Gly) ($46.0 \text{ kcal mol}^{-1}$) via iodination with HOI favors the formation of OH-Tyr-Gly over I-Tyr-Gly. Unexpectedly, mass spectrometry experiments detected I-Tyr-Gly but not OH-Tyr-Gly, suggesting that I-Tyr-Gly formation cannot be attributed to HOI alone. To clarify this result, we examined the thermodynamic role of the most reactive iodine species H_2OI^+ in the formation of aromatic I-DBPs under chloramination. Computational modeling of thermodynamic results shows that the formation of a loosely bonded complex of aromatic compounds with H_2OI^+ is the key step to initiate the iodination process. When H_2OI^+ serves as an acid catalyst and an iodinating agent, with HOI or H_2O acting as a proton acceptor, the energy barrier of I-DBP formation was significantly lower (10.8 – $13.1 \text{ kcal mol}^{-1}$). Therefore, even with its low concentration, H_2OI^+ can be involved in the formation of I-DBPs. These results provide insight into the mechanisms of aromatic I-DBP formation and important information for guiding research toward controlling I-DBPs in drinking water.

KEYWORDS: disinfection byproducts (DBPs), iodination pathway, thermodynamic modeling, LC-MS



INTRODUCTION

Drinking water disinfection is the most effective measure for prevention of water-borne diseases. While disinfection inactivates microbial pathogens, disinfectants inevitably react with organics in source water to produce a variety of disinfection byproducts (DBPs).¹ Epidemiological studies have observed a potential association of DBP exposure with the increased risk of developing bladder cancer, pregnancy abnormalities, and other adverse health effects.² More than 700 halogenated DBPs have been identified; however, it remains unclear which DBPs cause the observed adverse outcomes. Efforts to reduce regulated DBPs have also resulted in some unintended consequences. For example, switching from chlorination to chloramination can significantly reduce regulated DBPs (e.g., trihalomethanes (THMs) and haloacetic acids (HAAs)). Unfortunately, chloramination has been linked to the increased formation of some unregulated DBPs, including nitrosodimethylamine (NDMA) and iodinated DBPs (I-DBPs).^{3,4} Some of the unregulated DBPs have shown higher cyto- and genotoxicity than the regulated DBPs by several orders of magnitude.^{1,5–8} Particularly, I-DBPs generally show much higher genotoxicity, cytotoxicity, and

developmental toxicity than their chloro- (Cl-DBPs) and bromo- (Br-DBPs) analogues;^{9–12} I-DBPs have been frequently detected in disinfected waters at concentrations from ng L^{-1} to $\mu\text{g L}^{-1}$.^{7,8}

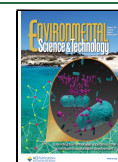
Existing studies have mainly focused on aliphatic I-DBPs, especially I-THMs and I-HAAs.^{13–16} However, aromatic I-DBPs show 50–200 times higher developmental toxicity and growth inhibition than aliphatic I-DBPs^{11,17} and other known I-DBPs.^{10,18} Using the precursor ion scan method, numerous aromatic I-DBPs have been detected in chloraminated waters, tap water, and cooking water.^{8,9,11,18,19} For instance, aromatic I-DBPs (e.g., 2,4,6-triiodophenol and 2,6-diiodo-4-nitrophenol) were widely detected in finished drinking water samples from China with concentrations up to 31 ng L^{-1} .^{18,20} Therefore, understanding the formation of I-DBPs, specifically

Received: August 16, 2021

Revised: December 30, 2021

Accepted: January 5, 2022

Published: January 21, 2022



aromatic I-DBPs, remains an important topic of research. Recent studies have identified aromatic peptides as precursors to several aromatic I-DBPs (e.g., 3-iodo-tyrosylalanine, 3-iodo-tyrosylglycine (3-I-Tyr-Gly), 3,5-diiodo-tyrosylalanine, and 3,5-diiodo-Tyr-Gly).²¹ However, the formation mechanisms of aromatic peptide I-DBPs are unclear. Therefore, we applied computational modeling to explore the formation mechanisms of I-peptides under chloramination of aromatic dipeptides, starting with Tyr-Gly, in the presence of iodide (I^-).

Hypiodous acid (HOI) is generally considered as the predominant iodinating agent and is generated from the oxidation of iodide (I^-) under chloramination conditions.²² HOI can react with aromatic compounds such as phenols to form I-DBPs.¹³ The formation of aromatic I-DBPs is often explained via electrophilic substitution on the aromatic group (S_EAr) (Scheme S1). This mechanism involves the initial formation of a π -complex via halogen addition, followed by a σ -complex (arenium ion) intermediate, and finally, the formation of I-DBPs via loss of a proton from its ipso-position. In the classic multistep S_EAr reaction, iodination is required for the halogen addition that is commonly accepted as the rate-controlling step rather than a deprotonation reaction. In this case, the primary hydrogen–deuterium kinetic isotope effects ($KIEs = k_H/k_D$, Section S1 and Scheme S2) are not typically observed in S_EAr reactions, which lead to the conclusion that deprotonation of the σ -complex is not involved in the rate-controlling step.^{23–25} However, previous studies have also shown that this mechanism cannot explain iodination of several aromatic compounds due to their primary KIE (k_H/k_D), including 1.47–2.06 for dimethenamid,²⁵ 3.8 for 2,4,6-trideuterioanisole,²⁶ 3.97 for 2,4,6-trideuterophenol,²⁷ 2.3–5.4 for 4-nitrophenol,²⁸ and 4.4 for Ni(II)-coordinated pyrazole.²⁹ Additionally, the σ -complex intermediate was not observed in the formation of aromatic I-DBPs.³⁰ These observations suggest that iodination exhibits unique characteristics compared to other S_EAr reactions. This leads us to further study the mechanisms of the formation of iodinated DBPs.

HOI is considered to be an active iodinating agent; however, a few recent studies have found that the presence of hypiodous acidium ion (H_2OI^+) is significant.^{25,31,32} H_2OI^+ could be formed via protonation of HOI (Scheme S3), and its concentration primarily depends on the pH, total iodine (+I) concentrations, and to some extent chloride concentration.^{33,32} A recent kinetic study of the iodination of dimethenamid revealed that HOI was insignificant in the production of the iodinated product and instead found that H_2OI^+ was the predominant active iodinating agent.³² An earlier study of aromatic iodination showed that H_2OI^+ was only significant under highly acidic conditions ($pH < 3.5$).¹³ Further, several earlier studies have reported H_2OI^+ as a more active iodinating agent than HOI.^{26,32,34,35} This led us to examine the thermodynamic role of H_2OI^+ in the mechanisms of aromatic I-dipeptide DBP formation.

Peptides occur in numerous species and large amounts in water. Our group has previously identified over 600 chemical signatures of peptides in drinking water, and many of them correspond to tyrosine-containing peptides.³⁶ A series of dipeptides have been detected in source water at the $\mu g L^{-1}$ level. For instance, the concentrations of Tyr-Gly, tyrosylglycine (Tyr-Ala), and phenylalanyl-glycine (Phe-Gly) in raw water were 1.1, 1.0, and 2.0 $\mu g L^{-1}$, respectively.³⁷ These peptides would pass through drinking water pretreatment and react with disinfectants to form I-DBPs. Therefore, in the

present study, we selected dipeptides Tyr-Gly, Tyr-Ala, glycylytyrosine (Gly-Tyr), and Phe-Gly as model precursors of aromatic I-DBPs because they are ubiquitous in source water.³⁶

We examined their iodination reactions in the presence of HOI, H_2OI^+ , and ICl using density functional theory (DFT) calculation. Furthermore, experiments were carried out in simulated chloraminated water to identify the formation of aromatic I-DBPs from Tyr-Gly. The results are important for the understanding of the formation mechanism of aromatic I-DBPs, providing necessary information for better control of aromatic I-DBPs in treated water.

MATERIALS AND METHODS

Computational Details. All quantum chemical calculations were performed using the Gaussian 09 program.³⁸ The geometry of the reactants, products, and transition states (TSs) was fully optimized with hybrid density functional theory (DFT) using the M06-2X functional.³⁹ The effective core potential LANL2DZ basis set was applied for iodine atoms, and the basis set of 6-31+G(d) was used for the remaining atoms, including C, H, O, and N. Table S1 shows the calculated results using different methods (M062X-D3, M06-2X, B3LYP, wB97XD, and MPW1PW91), and the corresponding discussion is presented in Section S2. The water solvent was introduced by the continuum solvation model SMD.⁴⁰ The vibrational frequency calculations were carried out to identify the stationary points (without imaginary frequency) or transition states (with only one imaginary frequency), as well as to obtain the thermodynamic contributions. Furthermore, intrinsic reaction coordinate (IRC) theory was used to confirm the accurate connectivity of the transition states toward both the reactant and product. The profiles of free energies (PFEs) including the effects of both enthalpic and entropic factors were established by calculating the additional single-point energy at a more flexible basis set on the optimized structures. That is, iodine was performed with the LANL2DZ basis set, and the remaining atoms were treated with 6-311+G(3df,2p) level basis sets. All free energies were calculated at 298.15 K and 1 atm. We calculated the reaction rate constant (k) with transition-state theory (TST) based on the PFE calculation results, and the solvent cage effect was included to simulate the realistic solution.⁴¹ Details of the expressions are described in Section S2. The reaction rate is the product of the rate constant and reactant concentrations.

Chloramination Experiment. As previously reported,²¹ monochloramine solution was freshly prepared before use. First, ammonium chloride was dissolved in a bicarbonate buffer solution (10 mM, $pH = 8.5$). Next, the sodium hypochlorite solution was added dropwise into the ammonium chloride solution under stirring in an ice–water bath. The molar ratio of Cl to N was maintained at 0.7:1 to minimize the formation of dichloramine and ensure that NH_2Cl was predominant. The mixture was allowed to react and equilibrate for 1 h under stirring in the ice–water bath, before use.

Tyr-Gly solution (25 μM) was prepared with phosphate buffer (10 mM, $pH 7$). Monochloramine (50 μM), freshly prepared, was spiked with 1 μM KI dropwise under stirring and further allowed to react for 30 min under stirring to ensure the oxidation of KI to HOI.³² Next, the Tyr-Gly solution (100 mL) and the monochloramine solution containing HOI (100 mL) were mixed for the iodination reaction. Controlled reactions were performed in phosphate buffer (10 mM), including chloramination of Tyr-Gly without iodide and Tyr-

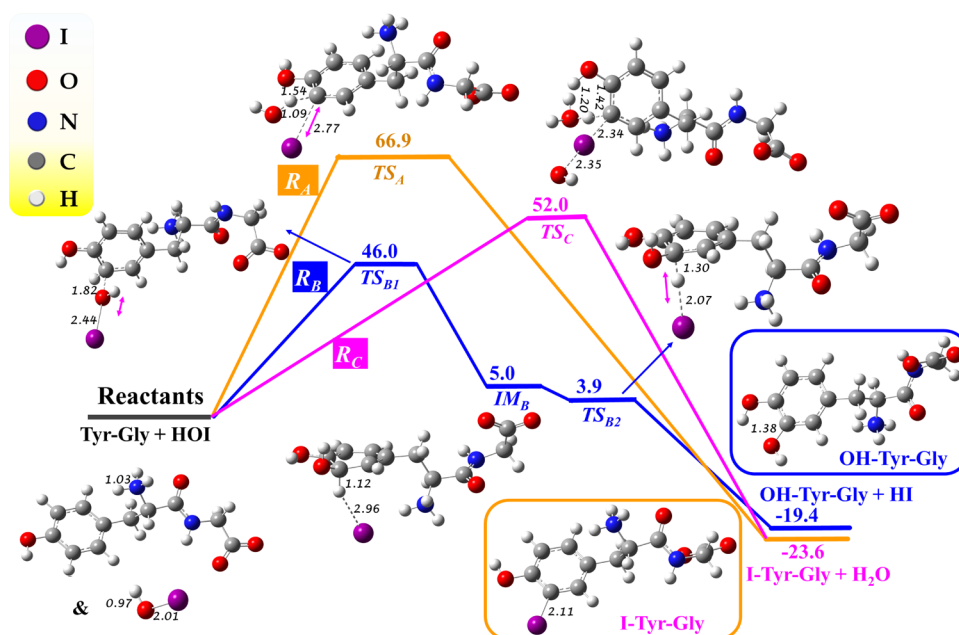


Figure 1. Free energy surface of the Tyr-Gly reaction with HOI by the I-atom attack route (R_A , orange line) and O-atom attack (R_B , blue line) route, as well as the involvement of the solvent water molecule (R_C , pink line) (energy in kcal mol⁻¹ and bond length in Å).

Gly in the presence of iodide without chloramination. After the mixture reacted in the dark at room temperature for set time intervals, an aliquot of 0.5 mL of FA was added to each reaction solution (0.25% FA) to quench the reaction via the FA reaction with monochloramine.⁴² The initial and residual monochloramine concentrations were measured using the chlorine amperometric titrator. Experimental materials and SPE extraction are listed in Section S3.

High-Resolution Mass Spectrometry Analysis. A quadrupole time-of-flight mass spectrometer (Sciex QTOF x500R) equipped with an electrospray ionization (ESI) source was used to determine the accurate masses of parent and product ions of Tyr-Gly and its iodinated products under chloramination conditions. The mass spectrometry experiments were performed in positive mode, and the parameters were set as follows: ion spray voltage, 5500 V; temperature, 0 °C; declustering potential, 80 V; gas 1 (spray gas, N₂), 25 arbitrary units; gas 2 (heat conduction gas, N₂), 0 arbitrary units; curtain gas (N₂), 25 arbitrary units; collisionally activated dissociation gas, 7 arbitrary units; scan range, 100–800 *m/z*; and accumulation time, 250 ms. The SPE eluents were injected by direct infusion at a flow rate of 7 μL min⁻¹, and the MS and MS/MS spectra were acquired. Sciex OS version 1.4 was used for instrument control and data analysis.

HPLC-MS/MS (MRM) Method. LC separation was performed on an Agilent 1290 series LC system with a Luna C18(2) column (100 mm × 2.0 mm i.d., 3 μm particles; Phenomenex, Torrance, CA). Mobile phases A and B were H₂O/ACN (95/5, v/v, 0.1% FA) and ACN (0.1% FA), respectively. The flow rate was 300 μL min⁻¹, and the injection volume was 1 μL. The gradient elution program was (corresponding to B) as follows: 0–10 min, 0–60%; 10–10.1 min, 60–100%; 10.1–12 min, 100%; 12–12.1 min, 100–0%; and 12.1–15 min, 0%. MS/MS (MRM) quantification was performed on a Sciex QTRAP 5500 triple quadrupole ion-trap tandem mass spectrometer. The mass spectrometer parameters were optimized as follows: positive mode, ion spray voltage, 5500 V; source temperature, 500 °C; gas 1 (50 arbitrary

units); gas 2 (40 arbitrary units); curtain gas (30 arbitrary units); and accumulation time for each ion pair, 250 ms. The ion-pair transitions for each compound and the corresponding parameters are listed in Table S2. Analyst version 1.5 was used for instrument control and data analysis. The extracted ion chromatograms of each compound are presented in Figure S1.

RESULTS AND DISCUSSION

Theoretical Calculation on Tyr-Gly Reactions with HOI. HOI as the predominant iodinating agent is widely accepted as responsible for I-DBP formation in chloraminated water.³² Using computational modeling, we first examined two possible competing processes of Tyr-Gly reacting with HOI, including I-atom attack (R_A) and O-atom attack (R_B) routes. Figure 1 illustrates the free energy surfaces of R_A and R_B routes, which were obtained after full optimization of all related intermediates, transition states, and products. Details of the definitions are described in Section S4. The R_A route shows the direct I-substitution of Tyr-Gly by HOI via a single concerted transition state (TS_A) [HOI⋯Tyr-Gly] with a barrier of 66.9 kcal mol⁻¹, leading to the formation of I-Tyr-Gly. This route is an exothermic process with a negative reaction energy (−23.6 kcal mol⁻¹). The R_B route presents the O-attack reaction mechanism with a stepwise addition–elimination pathway (Figure 1). The oxidation of Tyr-Gly starts with a π -addition that connects the O atom of HOI to the unsubstituted C atoms of Tyr-Gly via a transition state (TS_{B1}) [I(H)O⋯Tyr-Gly] with a barrier of 46.0 kcal mol⁻¹, forming a hydroxylated intermediate (IM_B). Subsequently, IM_B is vibrationally excited to easily form a hydroxylated product OH-Tyr-Gly. The energy barriers indicate that the initial step of π -addition is rate-limiting via the stepwise route R_B . The energy barrier of the O-attack route R_B is 20.9 kcal mol⁻¹ lower than that of the concerted I-attack route R_A . Thus, the stepwise route R_B is energetically favored over the concerted route R_A to form OH-Tyr-Gly from the reaction of Tyr-Gly with HOI.

Route R_C (Figure 1) considers the involvement of the solvent water molecule acting as a weak base for the leaving

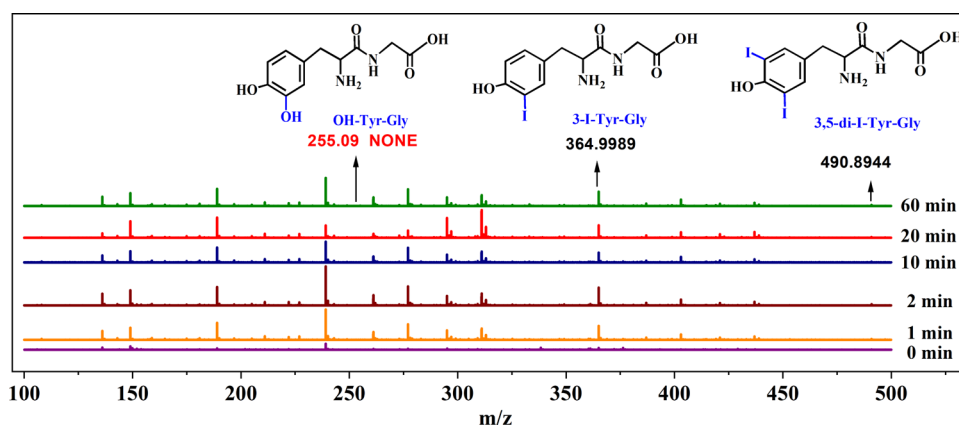


Figure 2. Full-scan high-resolution mass spectra of Tyr-Gly during the chloramination of a solution containing iodide.

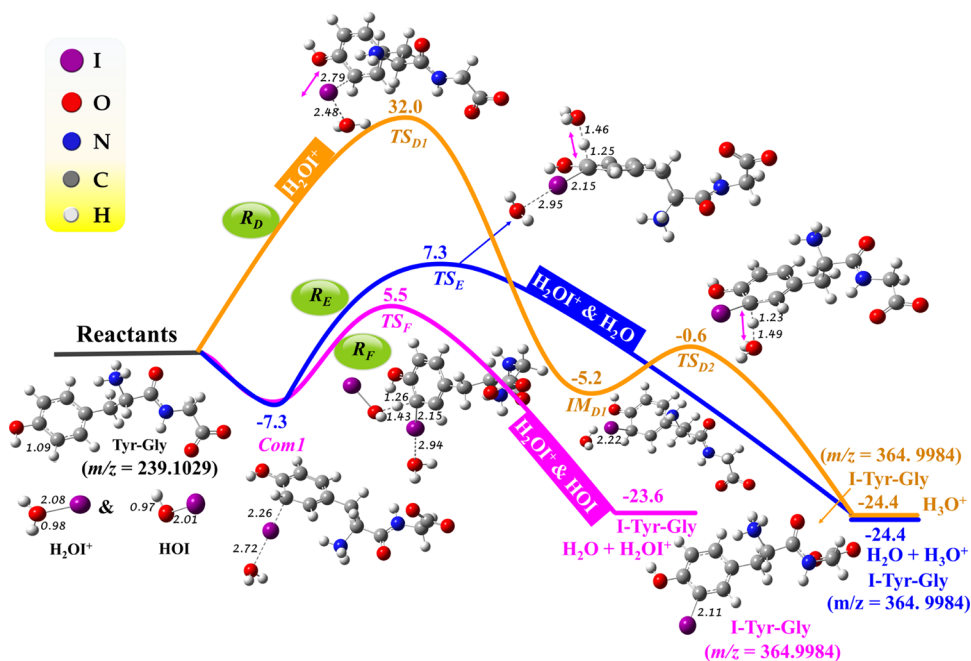


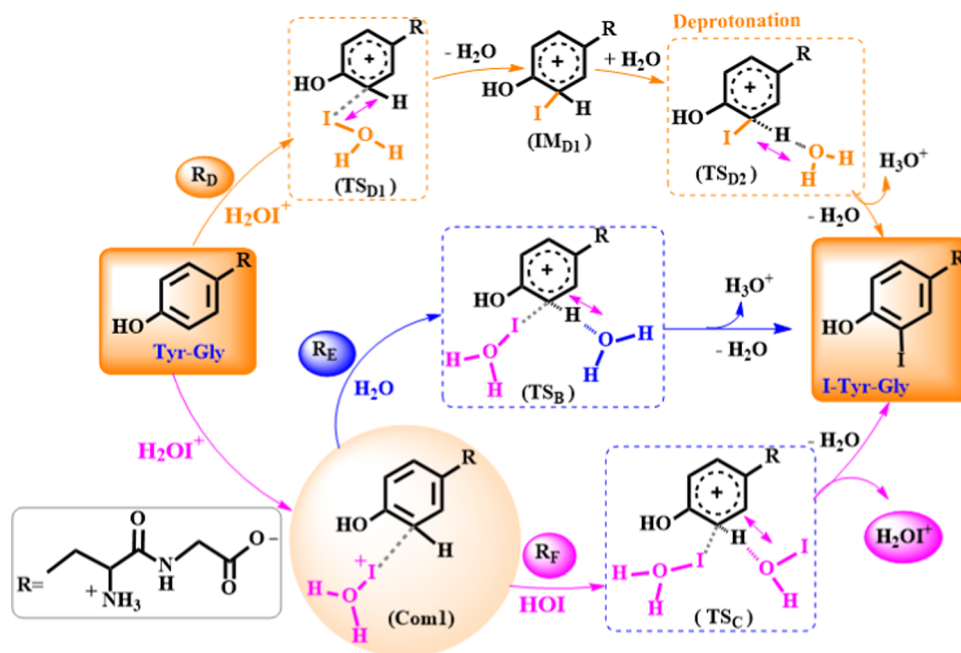
Figure 3. Free energy surface of the Tyr-Gly reaction with H_2OI^+ . R_D : the addition–elimination pathway of H_2OI^+ alone (orange line); R_E : the pathway via a water-assisted reaction (blue line); R_F : the pathway via an HOI-assisted reaction (pink line) (units: energy in kcal mol^{-1} and bond length in Å).

proton based on previous reports.^{25,30,43} The direct I-substitution of Tyr-Gly by HOI could occur via a single concerted transition state (TS_C) [$\text{HOI}\cdots\text{Tyr-Gly}\cdots\text{H}_2\text{O}$] to form I-Tyr-Gly. The energy barrier of this route R_C ($52.0 \text{ kcal mol}^{-1}$) is $6.0 \text{ kcal mol}^{-1}$ higher than that of the stepwise route (R_B), favoring the O-attack route R_B . This suggests that OH-Tyr-Gly should be the dominant product instead of I-Tyr-Gly in the HOI and Tyr-Gly reaction. Two previous studies showed that the bond energy of C–I in $\text{C}_6\text{H}_5\text{I}$ ($272.0 \text{ kJ mol}^{-1}$) is lower than that of C–OH in $\text{C}_6\text{H}_5\text{OH}$ ($463.6 \text{ kJ mol}^{-1}$).^{19,44} Thus, once OH-Tyr-Gly formed, it could be more stable than I-Tyr-Gly.

Experimental Identification of Iodinated Products.

To clarify the mechanism of the HOI reaction with Tyr-Gly, we performed experiments to identify the two products (I-Tyr-Gly and OH-Tyr-Gly) during chloramination of water containing Tyr-Gly and I^- . Although chlorinated products of Tyr-Gly were also produced under chloramination based on our previous studies,⁴⁵ the focus of this study was to elucidate

the iodination process. The reaction products were detected using a high-resolution mass spectrometer (Q-TOF). Both MS and MS/MS spectra of the products were obtained. Additionally, a control sample with Tyr-Gly and I^- in water without chloramine was also analyzed. Figure 2 shows the full-scan spectrum of the reaction solution after it was subtracted from the spectrum of the control sample. The formation of I-Tyr-Gly at m/z 364.9989 $[\text{M} + \text{H}]^+$ and the product 3,5-di-I-Tyr-Gly at m/z 490.8944 $[\text{M} + \text{H}]^+$ were detected, consistent with previous experimental results.²¹ The identification of the two iodinated products was confirmed by their precursor ions, isotopic patterns, and fragment ions, as shown in Figure S2-5 and Table S3-4. To evaluate the dynamics of the reactions, we developed an HPLC-MS/MS (MRM) method to monitor the iodinated products in the reaction solutions over time. Meanwhile, the corresponding residual monochloramine was measured using a chlorine amperometric titrator. As shown in Figure S6, the relative amounts of the two iodinated products and residual monochloramine reached equilibrium within 10

Scheme 1. Potential Reaction Routes for the Iodination of Tyr-Gly with H_2OI^+ ^a

^a R_D : the addition–elimination pathway of H_2OI^+ alone (orange line); R_E : the pathway via a water-assisted reaction (blue line); R_F : the pathway via an HOI-assisted reaction (pink line).

min, demonstrating the rapid iodination reactions of Tyr-Gly during chloramination. Unexpectedly, the characteristic spectrum of OH-DBP at m/z 255.09 was not observed during the reaction time from 1 min to 24 h. This suggests that OH-DBP is not formed or is below the detectable level. These MS results support the formation of I-Tyr-Gly but not HO-Tyr-Gly. This experimental observation is inconsistent with the calculation result for the Tyr-Gly reaction with HOI alone as described in Figure 1. Thus, the formation of I-Tyr-Gly cannot be attributed to the reaction of HOI alone, suggesting that different mechanisms may contribute to the formation of I-Tyr-Gly in the chloramination of water containing Tyr-Gly and I^- .

Iodination Reactions between Tyr-Gly and H_2OI^+ .

Based on recent experimental findings,³² we hypothesize that H_2OI^+ is a key active reactant to form aromatic I-DBPs. The calculated result shows that H_2OI^+ formation via a protonation reaction is a barrierless process (Section S5 and Figure S7). Therefore, we further examined the thermodynamics of the reactions between H_2OI^+ and Tyr-Gly to form aromatic I-Tyr-Gly under chloramination of water containing Tyr-Gly and I^- . Figure 3 shows the computational modeling of three possible routes (R_D , R_E , and R_F) of the reactions between Tyr-Gly and H_2OI^+ and their free energy surfaces. Scheme 1 depicts these pathways along with the complexes (intermediates), transition states, and products. Route R_D follows the classic electrophilic aromatic substitution ($S_E\text{Ar}$) mechanism with a stepwise addition–elimination pathway. This mechanism was proposed in the previous experimental research.³² H_2OI^+ directly attacks the phenyl ring of Tyr-Gly via a transition state (TS_{D1}) [$\text{H}_2\text{OI}^+\cdots\text{Tyr-Gly}$] with a barrier of 32.0 kcal mol⁻¹ (Figure 3), leading to the formation of a σ -adduct intermediate (IM_{D1}) [Tyr-Gly-I^+] and H_2O as a leaving group. This reaction is an exothermic process with a negative reaction energy (−5.2 kcal mol⁻¹). Subsequently, an H_2O molecule could also serve as the Brønsted base that deprotonates the intermediate IM_{D1} ,

producing H_3O^+ and the iodinated Tyr-Gly (I-Tyr-Gly) (Scheme 1), which requires overcoming a small energy barrier (4.6 kcal mol⁻¹) of the subsequent reaction (Figure 3). The energy barriers in route R_D indicate that the rate-limiting step is the initial electrophilic attack to form the σ -complex IM_{D1} , resulting in the formation of I-Tyr-Gly through the stepwise $S_E\text{Ar}$ mechanism.

In light of previous studies reporting that H_2O could be involved in the iodination processes,^{25,32} route R_E in Figure 3 examines the involvement of the solvent water molecule acting as a weak Brønsted base for the leaving proton in the H_2OI^+ and Tyr-Gly reaction. This reaction is a stepwise mechanism with fast formation of complex (Com1) [$\text{H}_2\text{OI}^+\cdots\text{Tyr-Gly}$] followed by a rate-controlling deprotonation reaction that resulted in the formation of I-Tyr-Gly. Surprisingly, Tyr-Gly and H_2OI^+ can easily form a loosely bonded complex (Com1) via an exergonic process (free energy of reaction: −7.3 kcal mol⁻¹) (Figure 3). On the contrary, the formation of complex [$\text{Tyr-Gly}\cdots\text{H}_2\text{O}$] is an endothermic process (4.0 kcal mol⁻¹, shown in Figure S8a). These data suggest that the complex (Com1) is energetically favorable. A subsequent reaction with H_2O via the transition state (TS_E) [$\text{H}_2\text{OI}^+\cdots\text{Tyr-Gly}\cdots\text{H}_2\text{O}$] can result in the formation of I-Tyr-Gly. Additionally, the solvent H_2O acted as a Brønsted base for the leaving proton to facilitate the iodination of Tyr-Gly with H_2OI^+ by considerably lowering the free energy of the transition states as compared to the process R_D . This solvent (water) effect on the substitution reaction is consistent with a previous study.⁴⁶ The energy barrier of the route R_E is 14.6 kcal mol⁻¹, which is approximately 17.4 kcal mol⁻¹ lower than that of the route R_D . Thus, the route R_E with a rate-controlling deprotonation reaction is energetically favored over the route R_D with iodine addition, resulting in the formation of I-Tyr-Gly. Accordingly, we concluded that H_2OI^+ could participate in the iodination mechanism before rate-controlling proton removal, which agrees with the experimental results in a previous study.²⁵

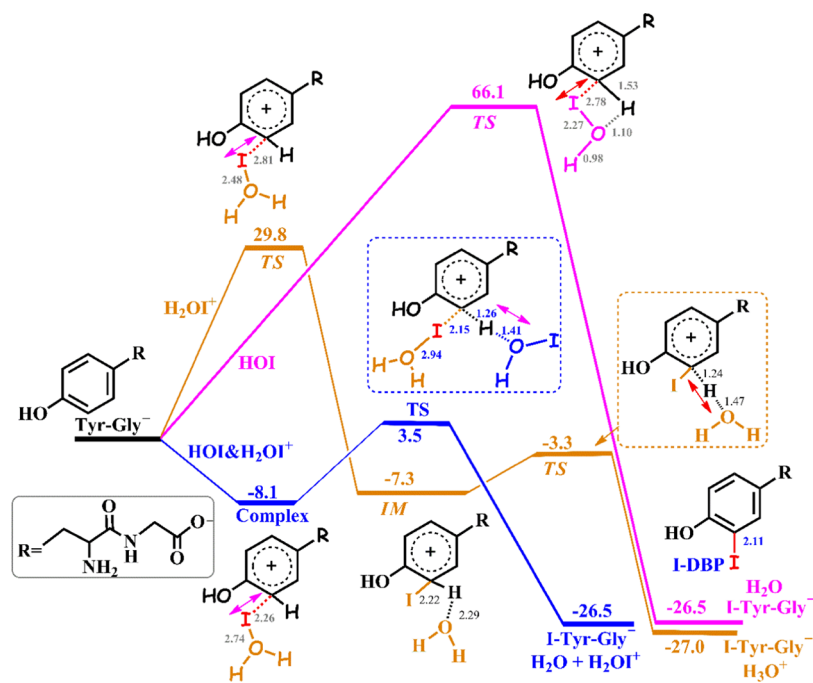


Figure 4. Free energy surface for the iodination of the anionic form Tyr-Gly[−]: (1) with HOI alone (pink line), (2) with H₂OI⁺ alone (orange line), and (3) involving H₂OI⁺ (blue line) as combined with HOI as the proton acceptor (units: energy in kcal mol^{−1} and bond length in Å).

Comparing the most favorable route for the Tyr-Gly and HOI reaction (R_B in Figure 1) with the Tyr-Gly and H₂OI⁺ reaction (R_E in Figure 3), the energy barrier of the H₂OI⁺ reaction route R_E is 31.4 kcal mol^{−1} lower than that of the HOI route R_B . Furthermore, the calculated rate constant of route R_E is 6.15×10^7 M^{−1} s^{−1}, and its reaction rate is 1.93×10^{-3} M s^{−1}, which is 23 orders of magnitude higher than that of the HOI reaction (route R_B). Although H₂OI⁺ in general has a relatively lower concentration than HOI, the reactivity of H₂OI⁺ is significantly higher than that of HOI, consistent with the previous experimental finding.³² Therefore, these findings show the significance of H₂OI⁺ as an acid catalyst and an iodinating agent in the formation of I-DBPs.

H₂OI⁺ Initiating the Iodination of Tyr-Gly with HOI. In light of H₂O acting as a proton acceptor to lower the energy barrier (route R_F in Figure 3 and Scheme 1), we then considered HOI as the proton acceptor based on HOI + H⁺ = H₂OI⁺. The formation of complex [Tyr-Gly⋯HOI] is predicted to be an endothermic process (free energy of reaction: 6.4 kcal mol^{−1}, shown in Figure S8b), while the formation of Com1 [Tyr-Gly⋯H₂OI⁺] is an exothermic process (−7.3 kcal mol^{−1}). Thus, Com1 [Tyr-Gly⋯H₂OI⁺] is thermodynamically favorable over [Tyr-Gly⋯HOI]. The concentration of Com1 [Tyr-Gly⋯H₂OI⁺] is estimated as 5.65×10^{-13} M (Section S6). The subsequent reaction of Com1 with HOI via the transition state (TS_F) can lead to the formation of I-Tyr-Gly. The energy barrier of route R_F is 12.8 kcal mol^{−1}, significantly lower than that of R_D , the iodination with H₂OI⁺ alone (32.0 kcal mol^{−1}), and R_E , the H₂OI⁺ reaction involving a water molecule (14.6 kcal mol^{−1}). Accordingly, the calculated rate constant of route R_F is 1.30×10^9 M^{−1} s^{−1}, which is close to that of a typical diffusion-controlled reaction (10⁹ M^{−1} s^{−1}). The reaction rate is 13 orders of magnitude larger than that of route R_D (9.67×10^{-6} M s^{−1}) without HOI as a proton acceptor. Further, when comparing the possible Brønsted bases (H₂O vs HOI), the

half-life is calculated as 8.0 h for route R_E (H₂O as the proton acceptor), while 0.4 h for route R_F (HOI as the proton acceptor). These data indicate that HOI as a proton acceptor would favor I-DBP formation. However, as solvent H₂O is much more abundant than HOI in the system, it can also contribute to the iodination of Tyr-Gly with a reaction rate constant of 6.15×10^7 M^{−1} s^{−1} in the reaction-controlled route R_E . Other proton acceptors such as a second Tyr-Gly molecule exist in the system, but some proton acceptors (e.g., OH[−]) do not participate in the rate-controlling step of iodination since the KIE is independent of pH.²⁵

Compared to route R_E , route R_F allows the release of H₂OI⁺, which can be recycled for the next iodination of Tyr-Gly. Due to the thermodynamic limitation, the H₂OI⁺ concentration is approximately 6–11 orders of magnitude lower than that of HOI in chloraminated water in a pH range of 6–10.³² The reaction rate is 7.35×10^{-10} M s^{−1} for route R_F , which is much higher than those of the reactions without complex formation, i.e., 5.23×10^{-42} M s^{−1} for route R_A and 2.42×10^{-23} M s^{−1} for route R_D . These data suggest that the formation of complex [Tyr-Gly⋯H₂OI⁺] facilitates the formation of I-Tyr-Gly, and route R_F is thermodynamically favored. Next, we considered the ICl reaction for the iodination of Tyr-Gly, and the calculation results are shown in Figure S9 and Table S6. This information is discussed in detail in Section S7. This result shows that compared to the most favorable pathway of the ICl reaction (route R_L in Figure S9), the energy barrier of the H₂OI⁺ reaction (route R_F) is lower by approximately 16.3 kcal mol^{−1}. The reaction rate constant of route R_F is higher than that of the ICl reaction (route R_L) by 12 orders of magnitude, and the reaction rate of the H₂OI⁺ reaction is 20 orders of magnitude higher than that of ICl. These data indicate that H₂OI⁺ has a higher reactivity than ICl for the formation of I-Tyr-Gly, which is also observed in the iodination of dimethenamid in a previous study.²⁵

pH Effect on Iodination Mechanisms. The iodination of dipeptides and the formation of I-DBPs could be affected by water pH. Previous research has reported pH values of 7.05–8.15 in raw water and 7.22–7.70 in treated drinking water in Beijing, China,⁴⁷ as well as 6.5–8.5 under typical drinking water treatment conditions. Accordingly, it is necessary to understand the iodination route in aqueous solutions at pH 6, 7, and 8. As shown in Figure S10, laboratory experiments demonstrated that the formation of the iodinated products decreased when the pH increased from 6 to 8. Similar iodination suppression by increasing pH has been reported in a previous study.²⁵ As indicated in previous studies,^{31,32} the decrease of the iodinated products cannot be ascribed to HOI, considering its consistent concentration at pH 6–8 when taking HOI disproportionation into account.^{31,32,22,32,48,49} Also, pH influence on the oxidation of KI to form HOI is not considered to be responsible for the decrease, since KI has been completely oxidized to HOI before the iodination reaction.^{22,32,49} Therefore, the pH effect on the reaction mechanisms of Tyr-Gly and H₂OI⁺ was further considered. Due to the three ionizable groups including carboxyl (–COOH), amino (–NH₂), and aromatic hydroxyl (–OH) groups,⁵⁰ Tyr-Gly has four dissociation forms (Figure S11 and the related discussion is provided in Section S8). Accordingly, it is necessary to understand the iodination route based on the dissociation forms of Tyr-Gly in aqueous solutions at realistic pH. Figure S12 shows that –COOH and –NH₂ groups of Tyr-Gly are mainly affected by pH, and the zwitterionic form (Tyr-Gly) and the anionic form (Tyr-Gly[–]) are the dominant species existing in the pH range of 6–8 in realistic raw water and drinking water. Particularly, in a water environment at pH 7, zwitterionic Tyr-Gly is the dominant species (90.9%) and minor Tyr-Gly[–] (9.1%). In a water sample of pH > 8, Tyr-Gly[–] begins to exceed Tyr-Gly. Thus, we further investigate the iodination mechanisms of Tyr-Gly[–] mediated by HOI alone, H₂OI⁺ alone, and H₂OI⁺ combined with HOI as the proton acceptor (Figure 4). The energy barrier is 11.6 kcal mol^{–1} in the iodination of Tyr-Gly[–] with HOI under H₂OI⁺ participation, lower than that without H₂OI⁺, namely, the Tyr-Gly[–] iodination mediated by HOI alone (66.1 kcal mol^{–1}) and by H₂OI⁺ alone (29.8 kcal mol^{–1}). Thus, H₂OI⁺ likely plays a significant role in the iodination of the anionic form Tyr-Gly[–].

Compared to Tyr-Gly, the anion Tyr-Gly[–] is more likely to form the complex [H₂OI⁺⋯Tyr-Gly[–]] under the H₂OI⁺ system, supported by its reaction free energy data (–8.1 kcal mol^{–1}). Furthermore, the energy barrier (11.6 kcal mol^{–1}) of the iodination of the Tyr-Gly[–] reaction is slightly lower than that of the iodination of the zwitterionic form Tyr-Gly (12.8 kcal mol^{–1}). These data suggest that the anion Tyr-Gly[–] could have a higher reactivity than the zwitterionic Tyr-Gly in iodination, which can possibly result in more I-Tyr-Gly formed at pH 8 than pH 6. Meanwhile, with the increase of pH, the predominant iodinating agent H₂OI⁺ decreases sharply and the formation of I-Tyr-Gly is supposed to decrease accordingly. However, as shown in Figure S10, the decreases of I-Tyr-Gly formation are much less than the theoretically predicted extent. A possible reason is that the increase of anion Tyr-Gly balanced the decrease of H₂OI⁺ in I-Tyr-Gly formation, suggesting the role of the anion Tyr-Gly in the iodination reactions when pH increases. Thus, the dissociation form of Tyr-Gly could not be responsible for the decrease of I-Tyr-Gly at pH 8, further confirming the important contribution of

H₂OI⁺ to I-Tyr-Gly formation. Although phosphate buffer has been observed to accelerate S_EAr iodination,⁵² the computational results support and evidence that such a kinetic influence did not compromise the mechanisms we proposed in this study.

Iodination of Other Aromatic Dipeptides Phe-Gly, Gly-Tyr, and Tyr-Ala. We also examined the iodination pathways of different aromatic dipeptides, including Phe-Gly, Gly-Tyr, and Tyr-Ala. Figures S13–S15 illustrate the PFE for iodination of the three dipeptides mediated by HOI alone, H₂OI⁺ alone, and H₂OI⁺ combined with HOI as the proton acceptor, respectively. Similar results are observed for the formation of iodinated DBPs generated from the calculated dipeptides under chloramination. For example, during the iodination of Phe-Gly (Figure S13), the energy barrier is predicted to be 13.1 kcal mol^{–1}, when H₂OI⁺ serves as the iodinating agent with HOI as the proton acceptor. This value is significantly lower than those of HOI alone (65.4 kcal mol^{–1}) and H₂OI⁺ alone (31.1 kcal mol^{–1}). Thus, the formation of iodinated Phe-Gly (I-Phe-Gly) is favored when H₂OI⁺ serves as the iodinating agent with HOI as the proton acceptor. A similar acid catalyst role of H₂OI⁺ was also observed in the iodination of dipeptides Gly-Tyr and Tyr-Ala (Figures S14 and S15).

Furthermore, by comparing the iodination of the calculated dipeptides, phenyl dipeptide (Phe-Gly) has a higher energy barrier of 13.1 kcal mol^{–1} than phenolic dipeptides, Tyr-Gly (12.8 kcal mol^{–1}), Gly-Tyr (8.1 kcal mol^{–1}), and Tyr-Ala (10.9 kcal mol^{–1}). Importantly, the formation of the H₂OI⁺ complex with Phe-Gly [H₂OI⁺⋯Phe-Gly] was less favorable since it was a less exothermic process (–1.6 kcal mol^{–1}) than with phenolic dipeptides (from –2.7 to –7.3 kcal mol^{–1}). The presence of an phenolic group (–OH) could facilitate the formation of the H₂OI⁺ complex, further enhancing the formation of I-DBPs. Thus, H₂OI⁺ could have a more significant role in iodination of the phenolic dipeptides than phenyl dipeptides, supported by a previous experimental observation.⁵¹

Environmental aromatic contaminants may often serve as DBP precursors. We have also examined iodination pathways of three aromatic contaminants: phenol (P) (Figure S16), *p*-methylphenol (MP) (Figure S17), and *p*-nitrophenol (NP) (Figure S18). Computational modeling clearly shows that the formation of I-P, I-MP, and I-NP thermodynamically favors the pathway of H₂OI⁺ serving as the iodinating agent with HOI as the proton acceptor over the other pathways of HOI alone or H₂OI⁺ alone. The energy barriers are comparable for the iodination of P (11.3 kcal mol^{–1}), MP (11.3 kcal mol^{–1}), and NP (11.4 kcal mol^{–1}). The calculated KIE ($k_{\text{H}}/k_{\text{D}}$) is 5.1 for P and 3.4 for NP, which are consistent with the experimental data in previous studies,^{52,28} further confirming the reliability of the computational modeling.

Environmental Implication. Recent studies have shown that aromatic I-DBPs have significantly higher toxicity than the regulated DBPs. Aromatic organic precursors and iodide widely exist in source water.^{53,54} Particularly, the concentration of iodide can be high in coastal region waters and industrial effluents, for example, saline groundwater, hydraulic fracturing effluent, and coal-fired power plant effluent.^{8,14} This study provides new insight into the understanding of aromatic I-DBP formation through H₂OI⁺ catalysis, providing important information to control and minimize toxic I-DBP formation in drinking water, wastewater treatment, and aquatic environment.

■ ASSOCIATED CONTENT

SI Supporting Information

The Supporting Information is available free of charge at <https://pubs.acs.org/doi/10.1021/acs.est.1c05484>.

Definition of the theoretical term; explanation of hydrogen isotope rationale; validation of the calculation method; calculation of rate constants, reaction rates, and complex concentrations; iodination reactions of ICl; different dissociation forms of Tyr-Gly in water; formation energies of complexes; extracted ion chromatograms of the iodinated products and their MRM parameters; HRMS identification of the iodinated products; relative amounts of the iodinated products and the residual monochloramine during chloramination over time; relative amounts of the iodinated products at different pH values; and free energy surfaces for the iodination of anionic form Tyr-Gly⁻, phenylalanyl-glycine, glycylytyrosine, tyrosylalanine, phenol, *p*-methylphenol, and *p*-nitrophenol (PDF)

■ AUTHOR INFORMATION

Corresponding Authors

Taicheng An – Guangdong Key Laboratory of Environmental Catalysis and Health Risk Control, Guangzhou Key Laboratory Environmental Catalysis and Pollution Control, School of Environmental Science and Engineering, Institute of Environmental Health and Pollution Control, Guangdong University of Technology, Guangzhou 510006, China; orcid.org/0000-0001-6918-8070; Phone: +86-20-39322298; Email: antc99@gdut.edu.cn

Xing-Fang Li – Division of Analytical and Environmental Toxicology, Department of Laboratory Medicine and Pathology, Faculty of Medicine and Dentistry, University of Alberta, Edmonton, Alberta T6G 2G3, Canada; orcid.org/0000-0003-1844-7700; Phone: 1-780-492-5094; Email: xingfang.li@ualberta.ca; Fax: 1-780-492-7800

Authors

Yanpeng Gao – Guangdong Key Laboratory of Environmental Catalysis and Health Risk Control, Guangzhou Key Laboratory Environmental Catalysis and Pollution Control, School of Environmental Science and Engineering, Institute of Environmental Health and Pollution Control, Guangdong University of Technology, Guangzhou 510006, China; Division of Analytical and Environmental Toxicology, Department of Laboratory Medicine and Pathology, Faculty of Medicine and Dentistry, University of Alberta, Edmonton, Alberta T6G 2G3, Canada; orcid.org/0000-0003-2156-8167

Junlang Qiu – School of Environmental Science and Engineering, Sun Yat-sen University, Guangzhou 510275, China; Division of Analytical and Environmental Toxicology, Department of Laboratory Medicine and Pathology, Faculty of Medicine and Dentistry, University of Alberta, Edmonton, Alberta T6G 2G3, Canada

Yuemeng Ji – Guangdong Key Laboratory of Environmental Catalysis and Health Risk Control, Guangzhou Key Laboratory Environmental Catalysis and Pollution Control, School of Environmental Science and Engineering, Institute of Environmental Health and Pollution Control, Guangdong University of Technology, Guangzhou 510006, China

Nicholas J. P. Wawryk – Division of Analytical and Environmental Toxicology, Department of Laboratory Medicine and Pathology, Faculty of Medicine and Dentistry, University of Alberta, Edmonton, Alberta T6G 2G3, Canada

Complete contact information is available at:

<https://pubs.acs.org/doi/10.1021/acs.est.1c05484>

Author Contributions

^{||}Y.G. and J.Q. contributed equally to this work.

Notes

The authors declare no competing financial interest.

■ ACKNOWLEDGMENTS

The authors thank the National Natural Science Foundation of China (41977365, 41888101, and 41731279), National Key Research and Development Program of China (2019YFC1804501), Local Innovative and Research Teams Project of Guangdong Pearl River Talents Program (2017BT01Z032), Natural Sciences and Engineering Research Council of Canada, the Canada Research Chairs Program, Alberta Innovates, and Alberta Health for their support. The authors thank the support from the National Supercomputer Center in Guangzhou. YG acknowledges the support of Guangdong University of Technology for her visiting scholarship.

■ REFERENCES

- (1) Li, X. F.; Mitch, W. A. Drinking Water Disinfection Byproducts (DBPs) and Human Health Effects: Multidisciplinary Challenges and Opportunities. *Environ. Sci. Technol.* **2018**, *52*, 1681–1689.
- (2) Diana, M.; Felipe-Sotelo, M.; Bond, T. Disinfection Byproducts Potentially Responsible for the Association between Chlorinated Drinking Water and Bladder Cancer: A review. *Water Res.* **2019**, *162*, 492–504.
- (3) Hua, G.; Reckhow, D. A. Comparison of Disinfection Byproduct Formation from Chlorine and Alternative Disinfectants. *Water Res.* **2007**, *41*, 1667–1678.
- (4) Plewa, M. J.; Muellner, M. G.; Richardson, S. D.; Fasano, F.; Buettner, K. M.; Woo, Y.-T.; McKague, A. B.; Wagner, E. D. Occurrence, Synthesis, and Mammalian Cell Cytotoxicity and Genotoxicity of Haloacetamides: An Emerging Class of Nitrogenous Drinking Water Disinfection Byproducts. *Environ. Sci. Technol.* **2008**, *42*, 955–961.
- (5) How, Z. T.; Kristiana, I.; Busetti, F.; Linge, K. L.; Joll, C. A. Organic Chloramines in Chlorine-Based Disinfected Water Systems: A Critical Review. *J. Environ. Sci.* **2017**, *58*, 2–18.
- (6) Muellner, M. G.; Wagner, E. D.; McCalla, K.; Richardson, S. D.; Woo, Y. T.; Plewa, M. J. Haloacetonitriles vs. Regulated Haloacetic Acids: Are Nitrogen-Containing DBPs More Toxic? *Environ. Sci. Technol.* **2007**, *41*, 645–651.
- (7) Richardson, S. D.; Plewa, M. J.; Wagner, E. D.; Schoeny, R.; DeMarini, D. M. Occurrence, Genotoxicity, and Carcinogenicity of Regulated and Emerging Disinfection By-products in Drinking Water: A Review and Roadmap for Research. *Mutat. Res., Rev. Mutat. Res.* **2007**, *636*, 178–242.
- (8) Liberatore, H. K.; Plewa, M. J.; Wagner, E. D.; VanBriesen, J. M.; Burnett, D. B.; Cizmas, L. H.; Richardson, S. D. Identification and Comparative Mammalian Cell Cytotoxicity of New Iodo-Phenolic Disinfection Byproducts in Chloraminated Oil and Gas Wastewaters. *Environ. Sci. Technol. Lett.* **2017**, *4*, 475–480.
- (9) Dong, H. Y.; Qiang, Z. M.; Richardson, S. D. Formation of Iodinated Disinfection Byproducts (I-DBPs) in Drinking Water: Emerging Concerns and Current Issues. *Acc. Chem. Res.* **2019**, *52*, 896–905.

- (10) Tian, D. Y.; Moe, B.; Huang, G.; Jiang, P.; Ling, Z. C.; Li, X. F. Cytotoxicity of Halogenated Tyrosyl Compounds, an Emerging Class of Disinfection Byproducts. *Chem. Res. Toxicol.* **2020**, *33*, 1028–1035.
- (11) Pan, Y.; Zhang, X. R.; Li, Y. Identification, toxicity and control of iodinated disinfection byproducts in cooking with simulated chlor(am)inated tap water and iodized table salt. *Water Res.* **2016**, *88*, 60–68.
- (12) Liu, J.; Zhang, X. Comparative toxicity of new halophenolic DBPs in chlorinated saline wastewater effluents against a marine alga: Halophenolic DBPs are generally more toxic than haloaliphatic ones. *Water Res.* **2014**, *65*, 64–72.
- (13) Bichsel, Y.; von Gunten, U. Formation of Iodo-Trihalomethanes during Disinfection and Oxidation of Iodide Containing Waters. *Environ. Sci. Technol.* **2000**, *34*, 2784–2791.
- (14) Richardson, S. D.; Fasano, F.; Ellington, J. J.; Crumley, F. G.; Buettner, K. M.; Evans, J. J.; Blount, B. C.; Silva, L. K.; Waite, T. J.; Luther, G. W.; McKague, A. B.; Miltner, R. J.; Wagner, E. D.; Plewa, M. J. Occurrence and Mammalian Cell Toxicity of Iodinated Disinfection Byproducts in Drinking Water. *Environ. Sci. Technol.* **2008**, *42*, 8330–8338.
- (15) Cancho, B.; Ventura, F.; Galceran, M.; Diaz, A.; Ricart, S. Determination, Synthesis and Survey of Iodinated Trihalomethanes in Water Treatment Processes. *Water Res.* **2000**, *34*, 3380–3390.
- (16) Ersan, M. S.; Liu, C.; Amy, G.; Plewa, M. J.; Wagner, E. D.; Karanfil, T. Chloramination of Iodide-Containing Waters: Formation of Iodinated Disinfection Byproducts and Toxicity Correlation with Total Organic Halides of Treated Waters. *Sci. Total Environ.* **2019**, *697*, No. 134142.
- (17) Yang, M.; Zhang, X. Comparative Developmental Toxicity of New Aromatic Halogenated DBPs in a Chlorinated Saline Sewage Effluent to the Marine Polychaete *Platynereis dumerilii*. *Environ. Sci. Technol.* **2013**, *47*, 10868–10876.
- (18) Pan, Y.; Li, W.; An, H.; Cui, H.; Wang, Y. Formation and occurrence of new polar iodinated disinfection byproducts in drinking water. *Chemosphere* **2016**, *144*, 2312–2320.
- (19) Liu, J.; Zhang, X.; Li, Y. Photoconversion of Chlorinated Saline Wastewater DBPs in Receiving Seawater is Overall a Detoxification Process. *Environ. Sci. Technol.* **2017**, *51*, 58–67.
- (20) Hu, S.; Gong, T.; Ma, J.; Tao, Y.; Xian, Q. Simultaneous determination of iodinated haloacetic acids and aromatic iodinated disinfection byproducts in waters with a new SPE-HPLC-MS/MS method. *Chemosphere* **2018**, *198*, 147–153.
- (21) Huang, G.; Jiang, P.; Blackstock, L. K. J.; Tian, D. Y.; Li, X. F. Formation and Occurrence of Iodinated Tyrosyl Dipeptides in Disinfected Drinking Water. *Environ. Sci. Technol.* **2018**, *52*, 4218–4226.
- (22) Bichsel, Y.; von Gunten, U. Oxidation of Iodide and Hypoiodous Acid in the Disinfection of Natural Waters. *Environ. Sci. Technol.* **1999**, *33*, 4040–4045.
- (23) Berliner, E. The current state of positive halogenating agents. *J. Chem. Educ.* **1966**, *43*, 124–133.
- (24) Zollinger, H. Hydrogen Isotope Effects in Aromatic Substitution Reactions. In *Advances in Physical Organic Chemistry*; Gold, V., Ed.; Academic Press, 1964; Vol. 2, pp 163–200.
- (25) Rose, M. R.; Reber, K. P. Kinetic Isotope Effects in Electrophilic Aromatic Halogenation of Dimethenamid in Chlor(am)inated Water Demonstrate Unique Aspects of Iodination. *Environ. Sci. Technol. Lett.* **2020**, *7*, 721–726.
- (26) Berliner, E. The Iodination of 2,4,6-Trideuterioanisole by Iodine Monochloride. *J. Am. Chem. Soc.* **1960**, *82*, 5435–5438.
- (27) Grovenstein, E.; Kilby, D. C. Kinetic Isotope Effect in the Iodination of 2,4,6-Trideuterophenol. *J. Am. Chem. Soc.* **1957**, *79*, 2972–2973.
- (28) Grovenstein, E.; Aprahamian, N. S. Aromatic Halogenation. II. The Kinetics and Mechanism of Iodination of 4-Nitrophenol and 4-Nitrophenol-2,6-d₂. *J. Am. Chem. Soc.* **1962**, *84*, 212–220.
- (29) Vaughan, J. D.; Smith, W. A. Kinetics of iodination of nickel(II)-coordinated pyrazole. *J. Am. Chem. Soc.* **1972**, *94*, 2460–2463.
- (30) Liljenberg, M.; Stenlid, J. H.; Brinck, T. Theoretical Investigation into Rate-Determining Factors in Electrophilic Aromatic Halogenation. *J. Phys. Chem. A* **2018**, *122*, 3270–3279.
- (31) Rose, M. R.; Lau, S. S.; Prasse, C.; Sivey, J. D. Exotic Electrophiles in Chlorinated and Chloraminated Water: When Conventional Kinetic Models and Reaction Pathways Fall Short. *Environ. Sci. Technol. Lett.* **2020**, *7*, 360–370.
- (32) Rose, M. R.; Roberts, A. L. Iodination of Dimethenamid in Chloraminated Water: Active Iodinating Agents and Distinctions between Chlorination, Bromination, and Iodination. *Environ. Sci. Technol.* **2019**, *53*, 11764–11773.
- (33) Schmitz, G. Inorganic reactions of iodine(+1) in acidic solutions. *Int. J. Chem. Kinet.* **2004**, *36*, 480–493.
- (34) Painter, B. S.; Soper, F. G. 68. Acid catalysis in the iodination of phenol. Iodination by acyl hypoiodites. *J. Chem. Soc.* **1947**, 342–346.
- (35) Berliner, E. Kinetics of the Iodination of Aniline. *J. Am. Chem. Soc.* **1950**, *72*, 4003–4009.
- (36) Tang, Y.; Xu, Y.; Li, F.; Jmaiff, L.; Hrudey, S. E.; Li, X.-F. Nontargeted identification of peptides and disinfection byproducts in water. *J. Environ. Sci.* **2016**, *42*, 259–266.
- (37) Huang, G.; Jmaiff Blackstock, L. K.; Jiang, P.; Liu, Z.; Lu, X.; Li, X.-F. Formation, Identification, and Occurrence of New Bromo- and Mixed Halo-Tyrosyl Dipeptides in Chloraminated Water. *Environ. Sci. Technol.* **2019**, *53*, 3672–3680.
- (38) Frisch, M. J.; Trucks, G. W.; Schlegel, H. B.; Scuseria, G. E.; Robb, M. A.; Cheeseman, J. R.; Scalmani, G.; Barone, V.; Mennucci, B.; Petersson, G. A.; Nakatsuji, H.; Caricato, M.; Li, X.; Hratchian, H. P.; Izmaylov, A. F.; Bloino, J.; Zheng, G.; Sonnenberg, J. L.; Hada, M.; Ehara, M.; Toyota, K.; Fukuda, R.; Hasegawa, J.; Ishida, M.; Nakajima, T.; Honda, Y.; Kitao, O.; Nakai, H.; Vreven, T.; Montgomery, J. A., Jr.; Peralta, J. E.; Ogliaro, F.; Bearpark, M. J.; Heyd, J.; Brothers, E. N.; Kudin, K. N.; Staroverov, V. N.; Kobayashi, R.; Normand, J.; Raghavachari, K.; Rendell, A. P.; Burant, J. C.; Iyengar, S. S.; Tomasi, J.; Cossi, M.; Rega, N.; Millam, N. J.; Klene, M.; Knox, J. E.; Cross, J. B.; Bakken, V.; Adamo, C.; Jaramillo, J.; Gomperts, R.; Stratmann, R. E.; Yazyev, O.; Austin, A. J.; Cammi, R.; Pomelli, C.; Ochterski, J. W.; Martin, R. L.; Morokuma, K.; Zakrzewski, V. G.; Voth, G. A.; Salvador, P.; Dannenberg, J. J.; Dapprich, S.; Daniels, A. D.; Farkas, Ö.; Foresman, J. B.; Ortiz, J. V.; Cioslowski, J.; Fox, D. J. *Gaussian 09*; Gaussian, Inc.: Wallingford, CT, USA, 2009.
- (39) Walker, M.; Harvey, A. J. A.; Sen, A.; Dessent, C. E. H. Performance of M06, M06-2X, and M06-HF Density Functionals for Conformationally Flexible Anionic Clusters: M06 Functionals Perform Better than B3LYP for a Model System with Dispersion and Ionic Hydrogen-Bonding Interactions. *J. Phys. Chem. A* **2013**, *117*, 12590–12600.
- (40) Marenich, A. V.; Cramer, C. J.; Truhlar, D. G. Universal Solvation Model Based on Solute Electron Density and on a Continuum Model of the Solvent Defined by the Bulk Dielectric Constant and Atomic Surface Tensions. *J. Phys. Chem. B* **2009**, *113*, 6378–6396.
- (41) Okuno, Y. Theoretical Investigation of the Mechanism of the Baeyer-Villiger Reaction in Nonpolar Solvents. *Chem. - Eur. J.* **1997**, *3*, 212–218.
- (42) Sharma, N.; Mishra, S. K.; Sharma, P. D. Kinetics and mechanism of oxidation of formic acid with chloramine-t in aqueous acidic medium. *Tetrahedron* **1990**, *46*, 2845–2856.
- (43) Galabov, B.; Nalbantova, D.; Schleyer, P. vR.; Schaefer, H. F. Electrophilic Aromatic Substitution: New Insights into an Old Class of Reactions. *Acc. Chem. Res.* **2016**, *49*, 1191–1199.
- (44) Liu, J.; Zhang, X.; Li, Y.; Li, W.; Hang, C.; Sharma, V. K. Phototransformation of halophenolic disinfection byproducts in receiving seawater: Kinetics, products, and toxicity. *Water Res.* **2019**, *150*, 68–76.
- (45) Jiang, P.; Huang, G.; Jmaiff Blackstock, L. K.; Zhang, J.; Li, X.-F. Ascorbic Acid Assisted High Performance Liquid Chromatography Mass Spectrometry Differentiation of Isomeric C-Chloro- and N-

Chloro-Tyrosyl Peptides in Water. *Anal. Chem.* **2017**, *89*, 13642–13650.

(46) Otto, R.; Brox, J.; Trippel, S.; Stei, M.; Best, T.; Wester, R. Single Solvent Molecules Can Affect the Dynamics of Substitution Reactions. *Nat. Chem.* **2012**, *4*, 534–538.

(47) He, X. Q.; Cheng, L.; Zhang, D. Y.; Li, W.; Xie, X. M.; Ma, M.; Wang, Z. J. First Molecular Detection of Group A Rotaviruses in Drinking Water Sources in Beijing, China. *Bull. Environ. Contam. Toxicol.* **2009**, *83*, 120–124.

(48) Bichsel, Y.; von Gunten, U. Hypoiodous acid: kinetics of the buffer-catalyzed disproportionation. *Water Res.* **2000**, *34*, 3197–3203.

(49) Kumar, K.; Day, R. A.; Margerum, D. W. Atom-transfer redox kinetics: general-acid-assisted oxidation of iodide by chloramines and hypochlorite. *Inorg. Chem.* **1986**, *25*, 4344–4350.

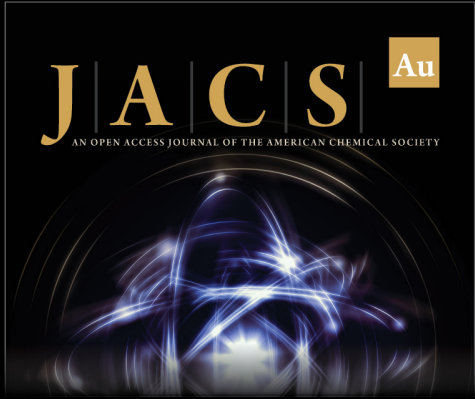
(50) Tominaga, T. T.; Imasato, H.; Nascimento, O. R.; Tabak, M. Interaction of Tyrosine and Tyrosine Dipeptides with Cu²⁺ Ions: A Fluorescence Study. *Anal. Chim. Acta* **1995**, *315*, 217–224.

(51) Huang, G.; Blackstock, L. K. J.; Jiang, P.; Liu, Z. S.; Lu, X. F.; Li, X. F. Formation, Identification, and Occurrence of New Bromo- and Mixed Halo-Tyrosyl Dipeptides in Chloraminated Water. *Environ. Sci. Technol.* **2019**, *53*, 3672–3680.

(52) Grovenstein, E.; Aprahamian, N. S.; Bryan, C. J.; Gnanaprasam, N. S.; Kilby, D. C.; McKelvey, J. M.; Sullivan, R. J. Aromatic halogenation. IV. Kinetics and mechanism of iodination of phenol and 2′6-dibromophenol. *J. Am. Chem. Soc.* **1973**, *95*, 4261–4270.

(53) Dong, H.; Qiang, Z.; Richardson, S. D. Formation of Iodinated Disinfection Byproducts (I-DBPs) in Drinking Water: Emerging Concerns and Current Issues. *Acc. Chem. Res.* **2019**, *52*, 896–905.

(54) Sharma, N.; Karanfil, T.; Westerhoff, P. Historical and Future Needs for Geospatial Iodide Occurrence in Surface and Groundwaters of the United States of America. *Environ. Sci. Technol. Lett.* **2019**, *6*, 379–388.



JACS Au
AN OPEN ACCESS JOURNAL OF THE AMERICAN CHEMICAL SOCIETY

 Editor-in-Chief
Prof. Christopher W. Jones
Georgia Institute of Technology, USA

Open for Submissions 

pubs.acs.org/jacsau  ACS Publications
Most Trusted. Most Cited. Most Read.